Electron attachment and detachment: C_6F_5Cl, C_6F_5Br, and C_6F_5I and the electron affinity of C_6F_5Cl

Thomas M. Miller* and A. A. Viggiano
Air Force Research Laboratory, Space Vehicles Directorate, Hanscom Air Force Base, Bedford, Massachusetts 01731-3010, USA
(Received 19 July 2004; published 4 January 2005)

Measurements are reported of rate constants for electron attachment to C_6F_5X (X=Cl, Br, I) and thermal electron detachment from $C_6F_5Cl^-$ over the temperature range 300–550 K in 133 Pa of He gas in a flowing-afterglow Langmuir-probe apparatus. This is the first case we know of where the parent anion has sufficiently low electron detachment energy that detachment (from $C_6F_5Cl^-$ in this case) has been observed in competition with a channel for dissociative electron attachment yielding a thermally stable anion (here, Cl^-). Because of this competition, it is shown that a simple mass spectrometric determination of the product branching fractions at long times will lead to erroneous results at elevated temperatures. The electron density profiles provide evidence for a new plasma decay process involving the detaching and nondetaching anions trapped in the space charge field of the positive ions. Electron attachment rate constants were found to be 1.0×10^{-7}, 1.1×10^{-7}, and 2.0×10^{-7} $cm^3\ s^{-1}$, at 300 K, for C_6F_5Cl, C_6F_5Br, and C_6F_5I, respectively, estimated accurate to ±25% except for C_6F_5I, where there is ±30% uncertainty. Rate constants for C_6F_5Cl changed little over our temperature range, while those for C_6F_5Br, and C_6F_5I increased with temperature. Electron detachment occurred only for $C_6F_5Cl^-$ in our temperature range. Detachment rate constants were immeasurable at room temperature but approached 4000 s^{-1} at 550 K. From these data the electron affinity (EA) for C_6F_5Cl was determined, EA (C_6F_5Cl) = 0.75 ± 0.08 eV. G3(MP2) calculations (based on Møller-Plesset perturbation theory) were carried out for the neutral and anion and yielded EA(C_6F_5Cl) = 0.728 eV.

DOI: 10.1103/PhysRevA.71.012702 PACS number(s): 34.80.Ht, 82.20.Pm, 52.27.Cm, 34.80.My

I. INTRODUCTION

We recently reported [1] on electron attachment to C_6F_6 and thermal detachment from $C_6F_6^-$. That project was carried out because our apparatus seemed a natural for a thorny attachment-detachment problem with a contentious history, but the experiment turned out to be interesting mainly because of the large symmetry change between neutral (D_{6h}) and anion (C_{2v})—the greatest of any system we know. The large entropy change between C_6F_6 and $C_6F_6^-$ resulted in inhibited electron detachment from what one would expect solely from the low electron affinity, EA(C_6F_6) = 0.53 ± 0.05 eV [1].

The present experiments were performed with the related molecules C_6F_5Cl, C_6F_5Br, and C_6F_5I, which do not undergo a large symmetry change: the neutrals are C_{2v} and the anions are C_s, resulting in a change in the rotational symmetry number from 2 to 1. For the present work this symmetry issue is relevant solely to C_6F_5Cl, the only one of the three molecules which has an EA low enough (0.82 ± 0.11 eV) [2] to permit electron detachment from the parent anion in the temperature range accessible to us (300–550 K). In the process, we discovered the first case (C_6F_5Cl) in which the attachment process yields both a detaching ion product ($C_6F_5Cl^-$) as well as nondetaching ones (Cl^- and possibly $C_6F_5^-$) in our temperature range:

$$e^- + C_6F_5Cl \leftrightarrow C_6F_5Cl^- \quad \Delta H = -0.8\ \text{eV} \tag{1a}$$

$$\rightarrow Cl^- + C_6F_5 \quad \Delta H = +0.2\ \text{eV} \tag{1b}$$

$$\rightarrow C_6F_5^- + Cl \quad \Delta H = +0.9\ \text{eV}. \tag{1c}$$

The reaction enthalpies at 298 K given in Eqs. (1) are from G3(MP2) and density functional calculations to be presented in Sec. VI below. The reaction enthalpies involving C_6F_5 are uncertain by 0.25 eV. One implication of thermal detachment from $C_6F_5Cl^-$ is that a simple mass spectrometric study of the ion products of attachment will yield incorrect product branching fractions. In the present work, the true branching fractions are determined by studying the electron density as a function of time. EA(C_6F_5Br) and EA(C_6F_5I) are too large (1.15 ± 0.11 and 1.45 ± 0.11 eV, respectively) [2] for the corresponding anions to detach electrons in our temperature range, and no detachment was observed.

We also found a new plasma decay effect related to the presence of detaching and nondetaching anions trapped in the space charge field of the plasma, with the detaching ones continually feeding fresh electrons into the milieu.

There have been relatively few studies of electron attachment to the C_6F_5X. Naff *et al.* studied the production of negative ions (and lifetimes) from C_6F_5X at 0–5 eV electron energy with a time-of-flight mass spectrometer [3]. Herd *et al.* used a flowing-afterglow Langmuir-probe (FALP) apparatus to measure electron attachment rate constants and branching fractions for the C_6F_5X in a weak thermalized plasma at 300 and 450 K [4]. Shimamori *et al.* used a pulsed radiolysis method to study electron attachment to C_6F_5X (including C_6F_6) at 300 K and 9.3 kPa Xe pressure as a function of mean electron energy [5]. Nakagawa has studied branching fractions from electron attachment to C_6F_5X using

*Electronic mail: thomas.miller@hanscom.af.mil

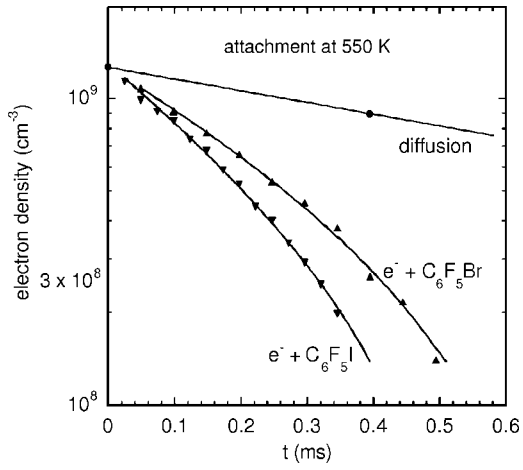

FIG. 1. An example at 550 K of attachment data for C_6F_5Br and C_6F_5I. The concentration of C_6F_5X was 1.05×10^{10} cm^{-3} in both cases. The upper line gives the ambipolar diffusion decay rate for the plasma, obtained in absence of reactant. The data show that C_6F_5I depletes the plasma electrons more efficiently than does C_6F_5Br.

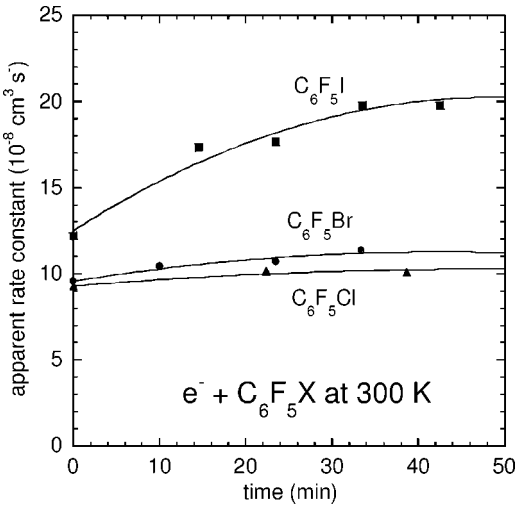

FIG. 2. An example at 300 K of the passivation problem for the C_6F_5X. The k_a reported here are those extrapolated to long measuring time.

negative chemical ionization mass spectrometry at very low pressures (4 mPa) [6].

II. EXPERIMENTAL METHOD

The FALP method [7] and the Air Force Research Laboratory apparatus [8] have been described in detail previously. An electron-He^+, Ar^+ plasma was established in a fast flow (100 m s^{-1}) of He buffer gas at 133 Pa pressure. C_6F_5X vapor was mixed in He gas at a typical concentration of 0.4% and added to the flowing plasma at point halfway down the length of the flow tube, yielding mixing ratios of C_6F_5X in the flow tube of 0.2–0.8 parts per million by volume. A movable Langmuir probe was used to measure the electron density (n_e) along the axis of the flow tube. Because the afterglow was continuous (not pulsed), data could be acquired over a long time (5 s per n_e datum) compared to the reaction time (ms). A mass spectrometer at the terminus of the flow tube was used to determine the ion products of attachment. The ambipolar diffusion decay constant ν_D was measured in the absence of C_6F_5X. We note that the plasma density in the electron attachment experiments was kept low enough that electron-ion and ion-ion recombination losses were completely negligible. With C_6F_5Br or C_6F_5I (and C_6F_5Cl at low temperature), the electron density data appeared as in Fig. 1. The fitted lines are from solutions to the one-dimensional rate equations for the coupled effects of diffusion and attachment on the electron density [7,8].

The C_6F_5X reagents were used as received from the supplier [9] aside from freeze-pump-thaw degassing cycles. The C_6F_5X vapors proved somewhat "sticky." The stickiness was manifested in three ways: (a) as mixtures were prepared, the pressure in the stainless steel vessel dropped with time until an equilibrium was reached with the walls of the vessel; (b) when the C_6F_5X was valved off from the FALP, it would take a minute for the electron density to return to its diffusion-limited value; and (c) the apparent electron attachment rate constant k_a increased in time as the reactant flow controller and feedline passivated. To minimize the effect of stickiness, the feedline was passivated with neat vapor prior to each data run, and apparent k_a were plotted versus measurement time. The reported result for k_a is that extrapolated to long time as shown in Fig. 2. The effect was minimal for C_6F_5Cl, small for C_6F_5Br, and large for C_6F_5I. The measured k_a are estimated to be accurate within ±25% for C_6F_5Cl and C_6F_5Br. For C_6F_5I, the measured k_a are estimated to be accurate to ±30% at all temperatures.

$C_6F_5Cl^-$ was found to undergo electron detachment at elevated temperatures. Electron detachment was evident in the data because the electron density initially decayed due to attachment, but at longer times approached a diffusion-limited slope, provided that the detachment rate constant k_d was sufficiently greater than the diffusion decay constant ν_D. The rate equations coupling the various processes are

$$\delta n_-/\delta t = k_a n_r n_e - k_d n_-, \tag{2}$$

$$\delta n_+/\delta t = -\nu_D n_+, \tag{3}$$

$$\delta n_e/\delta t = (\delta n_+/\delta t) - (\delta n_-/\delta t), \tag{4}$$

where n_-, n_+, n_e, and n_r are the anion, cation, electron, and neutral reactant concentrations, and the final equation expresses plasma neutrality. The equations are valid as long as $n_e > 0.1n_-$, in which case the more mobile electrons are responsible for diffusion of negative charge to the walls, while the anions are trapped in the space charge field of the cations [10]. The attachment data shown in Fig. 1 are governed by these rate equations with $k_d=0$, and the diffusion data in that figure correspond to $k_d=0$ and $n_r=0$.

Figure 3 shows C_6F_5Cl data at 467 K, where k_d is large enough to offset the effects of diffusion and then some. (If k_d were exactly equal to ν_D, the data in Fig. 3 would show a simple exponential decay rate governed solely by the attach-

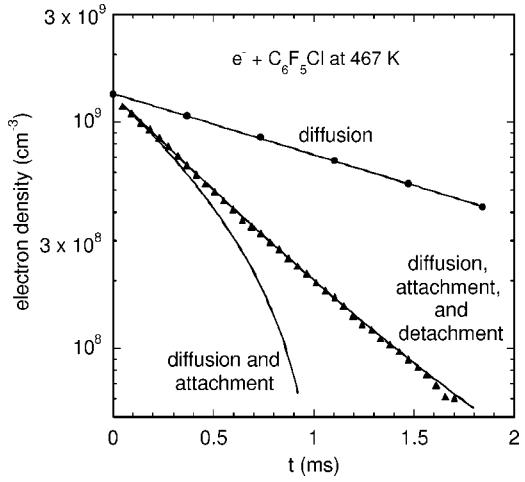

FIG. 3. Electron attachment-detachment data (points) for C_6F_5Cl at 467 K, for a C_6F_5Cl concentration of 1.38×10^{10} cm^{-3}. The fits to the data gave a diffusion decay constant of $\nu_D = 677$ s^{-1} (upper line) and $k_a = 9.3\times10^{-8}$ cm^{-3} s^{-1} and $k_d = 760$ s^{-1} (middle curve) and show little influence of nondetaching ion product of the reaction.

ment rate k_a.) At still higher temperatures, a new plasma effect was observed in the electron density plots: the diffusion-limited slope curved downward at long times, with a severity that increased with temperature. It was recognized, and confirmed in the mass spectra, that this effect was due to dissociative electron attachment producing ions with electron binding energies too high to detach at our temperatures—namely, Cl^- [EA(Cl)=3.613 eV] [11] and possibly (extremely little) $C_6F_5^-$ [EA(C_6F_5=3.4 eV] [12,13]. Figure 4 gives an example of the high-temperature C_6F_5Cl data, showing (a) the initial decay in electron density due to attachment, (b) the leveling off of the curve as attachment-detachment equilibrium for $C_6F_5Cl/C_6F_5Cl^-$ is nearly attained, and (c) the final diffusive death of the electron-ion plasma as the growth of the Cl^- (and possibly a very small amount of $C_6F_5^-$) product ions depleted the $C_6F_5Cl^-$ population which had been feeding electrons into the plasma. The branching fraction of nondetaching Cl^- product ions (0.14) in Fig. 4 is that which gave the best fit to the data. The fit is very sensitive to this fraction; changes of a few tenths of a percent cause obvious departures from an acceptable fit. In past work, without the complication of the nondetaching ions, it was straightforward to fit the attachment-detachment data, as the initial decay in the electron density is dependent on k_a, and the latter portion of the curve is dependent upon k_d/k_a. For C_6F_5Cl, a third parameter enters the picture—the branching fraction of nondetaching product ions—and affects the entire electron density curve. Thus, while this competition between detaching and nondetaching product ions is quite interesting, it carries with it a penalty in the accuracy with which k_a and k_d can be determined at elevated temperatures.

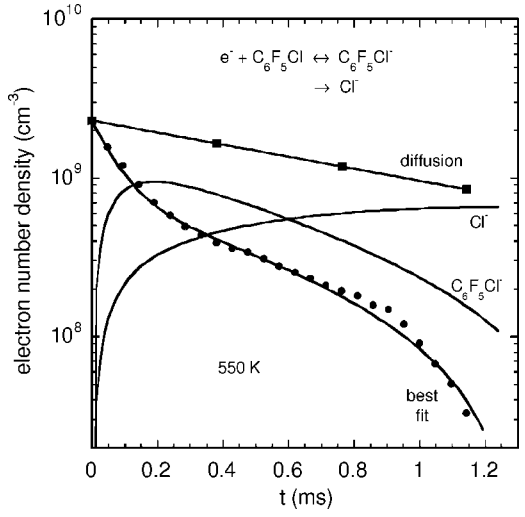

FIG. 4. Electron attachment-detachment data (points) for C_6F_5Cl at 550 K, for a C_6F_5Cl concentration of 8.49×10^{10} cm^{-3}. The ambipolar diffusion decay rate is $\nu_D = 869$ s^{-1} (upper line). The best-fit curve was obtained with $k_a = 1.0\times10^{-7}$ cm^{-3} s^{-1} and $k_d = 3880$ s^{-1} and a branching fraction for the $C_6F_5Cl^-$ ion product of 0.86 (lower curve).

III. ATTACHMENT AND DETACHMENT RESULTS

Rate constants k_a for electron attachment and the associated branching fractions measured in the present experiment are given in Table I. At 300 K, the electron attachment rate constants are 1.0×10^{-7}, 1.1×10^{-7}, and 2.0×10^{-7} cm^3 s^{-1}, for C_6F_5Cl, C_6F_5Br, and C_6F_5I, respectively. The formula given by Klots leads to collisional rate constants of 3.5, 3.5, and 3.6×10^{-7} cm^3 s^{-1}, respectively [14]. The measured rate constants for C_6F_5Cl change little with temperature in the range 300–550 K, while those for C_6F_5Br and C_6F_5I increase substantially. The increase in the attachment rate constants for C_6F_5Br may be described by an activation energy of 32 meV over the temperature range of the present experiment and analogously 77 meV for C_6F_5I.

Electron attachment to C_6F_5Cl was found to produce mainly the parent anion. Extremely low levels of $C_6F_5^-$ were observed, but the energetics given in Eq. (1) implies that the $C_6F_5^-$ is due to impurities. At elevated temperatures Cl^- was observed as a competing ion product. Figure 5 shows an Arrhenius plot for partial rate constants (the total rate constant multiplied by the branching fraction) for Cl^- production. The fitted line gives an estimate of the activation energy (which is likely an endothermicity) for Cl^- production—namely, 890 meV—though the data cover a very narrow temperature range. Points below 500 K were omitted from the fit because the branching fractions were $<1\%$ and thus unreliable.

Figure 6 shows an Arrhenius plot for partial rate constants for the production of Br^- from electron attachment to C_6F_5Br. The Br^- product is seen to increase with temperature in a manner described by an activation energy of $\sim$300 meV. The room-temperature point was omitted from this fit because the measured value of the branching fraction is so small ($<1\%$) that considerable uncertainty is involved.

Figure 7 shows an Arrhenius plot for the $C_6F_5^-$ ion product of attachment to C_6F_5I. The $C_6F_5^-$ channel is thought to be exothermic by 0.53 eV [12,15]. Since $C_6F_5^-$ is the major ion

TABLE I. Electron attachment rate constants k_a and ion product branching fractions measured in the present work for C_6F_5X, where X=Cl, Br, and I. For C_6F_5Cl the true branching fractions were determined from fits to the electron density plots accounting for loss of $C_6F_5Cl^-$ due to thermal detachment (see text), while the *apparent* branching fractions (in italics) were those observed with a mass spectrometer at 50 ms time. The $C_6F_5^-$ observed in the C_6F_5Cl attachment mass spectra may be due to impurities. The k_a are estimated accurate to within ±25% for C_6F_5Cl and C_6F_5Br and ±30% for C_6F_5I.

Molecule	T (K)	k_a (10^{-8} cm^3 s^{-1})	$C_6F_5X^-$ fraction	$C_6F_5^-$ fraction	X^- fraction
C_6F_5Cl	303	10.1	1	0	0
	383	9.8	1	0	0
			1.00	*0*	*<0.001*
	467	9.4	1	0	0
			0.95	*0.001*	*0.047*
	477	9.8	0.998	<0.001	0.002
			0.91	*0.003*	*0.093*
	487	9.4	0.997	<0.001	0.003
			0.85	*0.003*	*0.15*
	497	9.2	0.993	<0.001	0.007
			0.66	*0.006*	*0.33*
	507	10.5	0.97	<0.001	0.029
			0.49	*0.011*	*0.50*
	517	9.7	0.98	<0.001	0.020
			0.28	*0.012*	*0.71*
	527	10.4	0.948	0.001	0.051
			0.11	*0.019*	*0.87*
	537	9.5	0.943	0.001	0.056
			0.084	*0.022*	*0.89*
	550	10.0	0.871	0.002	0.13
			0.001	*0.018*	*0.98*
C_6F_5Br	299	11.1	0.99	0	0.007
	383	14.5	0.95	0	0.046
	467	17.0	0.82	0	0.18
	550	19.6	0.36	0	0.64
C_6F_5I	299	20.1	0.20	0.79	0.008
	383	26.3	0.048	0.94	0.009
	467	27.5	0.007	0.98	0.014
	550	31.8	0.002	0.99	0.010

product at all temperatures studied, the 37-meV activation energy indicated on the figure is assumed not to reflect an endothermicity, but rather to do with the competition between dissociative and nondissociative attachment. In any case, the activation energy deduced from Fig. 7 must be viewed as very approximate because the plotted line can hardly extend higher than shown: the branching fractions for the highest three points are 0.94, 0.98, and 0.99, and the total rate constant is nearing the collisional rate constant.

Table II presents electron detachment rate constants k_d for $C_6F_5Cl^-$ along with quantities needed to evaluate EA(C_6F_5Cl) from the attachment and detachment rate constants. In addition, the ambipolar diffusion decay constant ν_D (measured in absence of C_6F_5Cl) is listed for comparison to

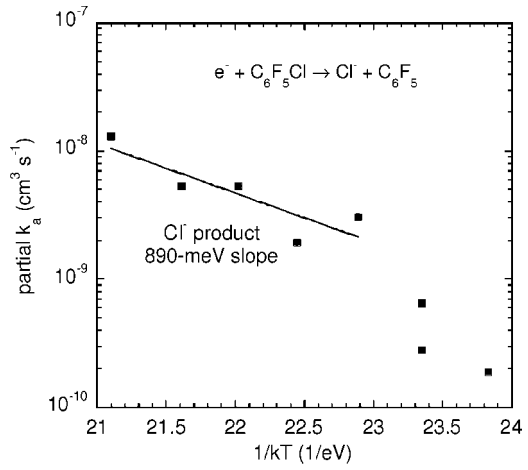

FIG. 5. Partial rate constants for the production of Cl^- in electron attachment to C_6F_5Cl.

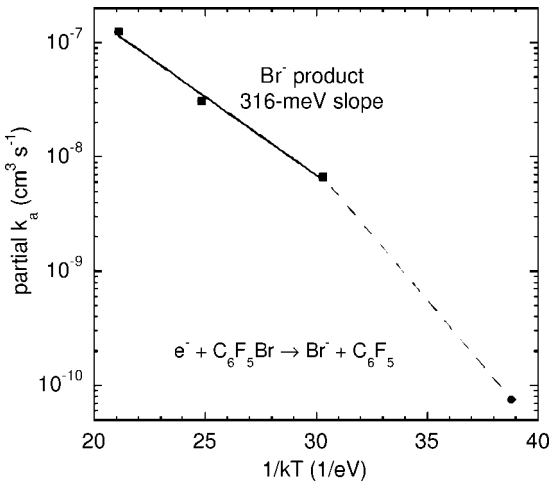

FIG. 6. Partial rate constants for the production of Br^- in electron attachment to C_6F_5Br.

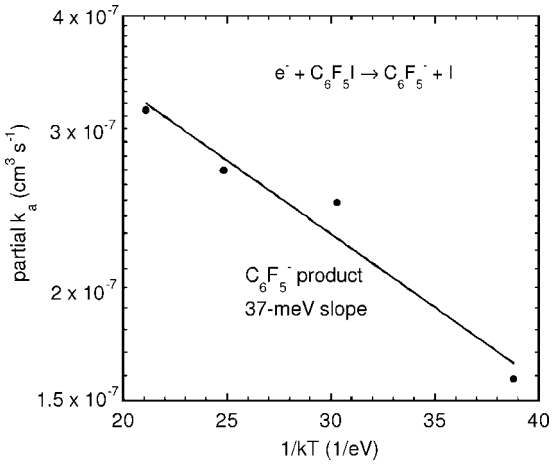

FIG. 7. Partial rate constants for the production of $C_6F_5^-$ in electron attachment to C_6F_5I.

TABLE II. Electron attachment rate constants k_a, detachment rate constants k_d, ambipolar diffusion decay constants ν_D, entropies S^o, integrated specific heats $\int C_p\, dT$, and apparent electron affinities EA, from the present work with C_6F_5Cl. The calculated values of S^o and $\int C_p\, dT$ in roman typeface are for neutral C_6F_5Cl, and those in italics are for the anion $C_6F_5Cl^-$. Values of ν_D may show variation at the same temperature because of deviations in the amount of Ar added and of slightly different plasma velocities. The k_a are estimated uncertain within 25% and the k_d within 35%. Those k_d given in parentheses are unreliable but give the best fit to the data.

T (K)	ν_D (s^{-1})	S^o (meV K^{-1})	$\int C_p\, dT$ (meV)	k_a (10^{-8} cm^3 s^{-1})	k_d (s^{-1})	EA (eV)
303	332	4.227	276.5	10.2	0	
		4.689	*306.1*	10.1	0	
383	486	4.638	410.2	9.7	(120)	
		5.120	*446.5*	9.8	(130)	
467	677	5.027	568.1	9.3	760	0.72
		5.524	*610.8*	9.5	780	0.72
477	682	5.071	587.9	9.8	1030	0.72
		5.569	*631.3*	9.8	1020	0.72
487	668	5.114	608.0	9.1	1155	0.73
		5.614	*652.0*	9.6	1110	0.72
497	672	5.157	628.2	9.4	1470	0.74
		5.658	*672.9*	9.1	1410	0.74
497	730	5.157	628.2	9.9	1530	0.74
		5.658	*672.9*	8.6	1570	0.73
507	720	5.199	648.6	10.5	2330	0.74
		5.702	*693.9*	10.5	2350	0.74
517	770	5.241	669.2	9.7	2230	0.75
		5.745	*715.2*			
527	769	5.282	689.9	10.3	2900	0.76
		5.788	*736.6*	10.51	3100	0.75
537	831	5.323	710.9	9.6	3550	0.76
		5.830	*758.2*	9.8	3340	0.76
				8.9	3220	0.76
				9.6	2750	0.77
550	869	5.376	738.3	10.1	(3880)	(0.77)
		5.884	*786.5*	9.8	(4400)	(0.77)

k_d values. Reliable values of k_d cannot be measured for $k_d < \nu_D$ because the plasma never reaches a steady-state condition at long times.

These results may be compared to those from an earlier FALP experiment carried out at 300 and 450 K in 133 Pa of He gas. At 300 K, Herd *et al.* [4] found attachment rate constants similar to ours for C_6F_5Cl and C_6F_5Br (8.4×10^{-8} and 8.3×10^{-8} cm^3 s^{-1}, respectively), but 6 times smaller for C_6F_5I (3.1×10^{-8} cm^3 s^{-1}), which we suspect is due to the severe passivation problem with C_6F_5I, as was illustrated in Fig. 2 (where even the first point at "$t=0$" comes after flowing neat C_6F_5I for 1 min). At 450 K, the rate constants of Herd *et al.* are within combined uncertainties compared to our results, except, again, for C_6F_5I. The branching fractions of Herd *et al.* are the same as ours for C_6F_5Cl at 300 and 450 K and the same for C_6F_5Br at 300 K, but lower at 450 K ($C_6F_5Br^-$ at ~0.60 vs 0.81), and the same for C_6F_5I at 450 K but higher at 300 K ($C_6F_5^-$ at $\geqslant$0.95 vs 0.79), with none of these discrepancies alarming. (The detachment rate for $C_6F_5Cl^-$ is far too small to affect the branching fractions below 450 K.)

Shimamori *et al.* [5] used the pulsed-radiolysis microwave-cavity technique to measure electron attachment rate constants for the C_6F_5X at 298 K in 9.3 kPa Xe gas. Microwave heating was used to vary the mean electron energy over the range 0.4–2.0 eV. Their 298 K rate constant for C_6F_5I agrees with ours, but those for C_6F_5Cl and C_6F_5Br are twice as large. The likely explanation for the difference (discounting possible experimental error) lies in the greater collisional stabilization efficiency of the 9.3 kPa of Xe buffer gas in the experiment of Shimamori *et al.* [5], versus our 133 Pa of He buffer gas.

Three decades ago, Naff *et al.* [3] used a time-of-flight mass spectrometer to study negative ions produced in the C_6F_5X by electrons in the 0–5 eV range. They used a retarding potential difference method to determine electron energies, with a resolution of ~0.1 eV. Autodetachment lifetimes for the $C_6F_5X^-$ were measured as 17.6, 20.8, and <1 μs for $X=$Cl, Br, and I, respectively. At their lowest electron energies ($\leqslant$0.1 eV) both X^- and $C_6F_5^-$ ion products were observed for each of the C_6F_5X, in addition to the parent anion in the C_6F_5Cl and C_6F_5Br cases. The differences with the

present work are likely due to the stabilization of the parent anion in He gas in our experiment, as well as the higher electron energies in the experiment of Naff *et al.*, as discussed by Herd *et al.* [4].

Aside from the attachment and detachment rate constants measured here, a consequential result of the present work is the demonstration that a purely mass spectrometric determination (at long times) of the ion products of electron attachment to C_6F_5Cl at elevated temperatures will be very misleading. As seen from Fig. 4 for 550 K, the plasma electrons have attached or diffused away in about 1.2 ms, having been replaced by Cl^- and a few remaining $C_6F_5Cl^-$. A mass spectrometer will indicate that the branching fraction of $C_6F_5Cl^-$ is very small—approximately 0.10—for times greater than 1.2 ms (after which the plasma is a positive-ion/negative-ion one). In fact, as Fig. 4 proves, the branching fraction for $C_6F_5Cl^-$ is actually 0.87 (the average of two such data) at 550 K. Table I lists both the true branching fractions, determined from fits to the electron density data, and apparent branching fractions (given in italics) obtained naively from the mass spectra.

Nakagawa used mass spectrometric determinations of branching fractions for electron attachment to the C_6F_5X and obtained results as predicted above for a simple mass spectrometric study—e.g., naming Cl^- as an 0.94 fractional product of attachment to C_6F_5Cl at 573 K and $C_6F_5Cl^-$ as only an 0.06 fractional product [6]. These branching fractions are very wrong; the results depend strongly on the reaction time because of thermal detachment from $C_6F_5Cl^-$. Nakagawa's branching fraction for attachment to C_6F_5I ($C_6F_5^-$, 1.0) is consistent with our observation of $\geqslant 0.95$. We find poorer agreement for C_6F_5Br: for example, we observe no $C_6F_5^-$ product, while Nakagawa reports 0.13–0.29 in the temperature range 423–573 K. Part of the problem may lie with Nakagawa's initial electron energy of 200 eV in a gas cell at $\sim$4 mPa.

IV. ELECTRON AFFINITY OF C_6F_5Cl

We have detailed in recent papers the procedure for deducing EA from the measured k_a and k_d [1,16]. This procedure uses the following equation, derived from the free energy for the attachment-detachment processes:

$$k_d = k_a L_0 (273.15/T) \exp\{[(\mathrm{EA})/kT] - (\Delta S^0/k) - (H_T - H_0)/kT\}. \quad (5)$$

In Eq. (5), k is Boltzmann's constant, L_0 is Loschmidt's number, EA is the electron affinity of C_6F_5Cl (at 0 K, by definition), ΔS^0 is the entropy change due to electron attachment at temperature T, and $H_T - H_0$ is the thermal energy correction needed to reduce the EA result from the measurement temperature T to 0 K. The entropy change was calculated for each T, as conveyed in Sec. VI, below, allowing the "EA" to be determined at temperature T. The integrated heat capacities contained in $(H_T - H_0)$ then allow this "EA" to be reduced to the true EA at 0 K. The calculated entropies and heat capacities for C_6F_5Cl neutral and anion are tabulated in Table II for each relevant temperature, along with the apparent EA deduced from each datum, using Eq. (5). The calculated quantities are of sufficient accuracy that the computational uncertainty is sub-meV [1], partly because the calculated quantities contribute only about 20% to EA. This fraction is greater for the C_6F_5Cl than for any molecule we have yet studied, because the difference between the entropies for the anion and neutral is so large that the net entropy change $[S(\mathrm{anion}) - S(\mathrm{neutral}) - S(\mathrm{electron})]$ is positive. Thus, the entropy and specific heat terms in Eq. (5) do not partially offset, as with earlier cases. Entropies and heat capacities for the electron were taken from the JANAF tables [17].

We did not simply average the apparent EA values in Table II to obtain a final result, but rather favored those at intermediate temperatures. The main reason is that the fitting procedure that yields k_a and k_d is most accurate when the attachment frequency ν_a $(=k_a/n_r)$ and k_d are comparable in magnitude (i.e., neither dominates the other), and k_d is greater than ν_D [10]. In the present work there is an additional reason to favor the intermediate-temperature results—namely, that the branching fraction for the dissociative product of attachment, Cl^-, is small ($\sim$2%), as given in Table I. For larger Cl^- branching fractions, the concentration of Cl^- ions will become large (see Fig. 4) since Cl^- does not undergo thermal detachment. At such point, it is more difficult to fit the data with the solution to our one-dimensional rate equations. The variation seen in the apparent EA's in Table II reflect this difficulty. For this same reason, we are assigning a larger-than-usual uncertainty to our EA value. The final result is $\mathrm{EA}(C_6F_5Cl) = 0.75 \pm 0.08$ eV. We suspect that the k_d values obtained above 500 K are too small as a result of the interference from the Cl^- product of attachment. To take the worst case, k_d at 550 K would have to be 9000 s^{-1} (instead of the average fitted value 4100) in order to make the apparent EA at that temperature equal to 0.75 eV. We do not know of measurements of k_d by others, with which to compare.

Dillow and Kebarle used ion equilibria in high pressure mass spectrometry to determine $\mathrm{EA}(C_6F_5Cl) = 0.82$ eV, $\mathrm{EA}(C_6F_5Br) = 1.15$ eV, and $\mathrm{EA}(C_6F_5I) = 1.41$ eV, all with an uncertainty of ± 0.11 eV [2]. $\mathrm{EA}(C_6F_5Cl) = 0.75$ eV ± 0.08 eV obtained in the present work agrees with that of Dillow and Kebarle, within experimental uncertainty. As will be seen below, G3(MP2) calculations (good to 0.1 eV in our experience [18] and often much better) give $\mathrm{EA}(C_6F_5Cl) = 0.728$ eV. A density functional method (Sec. VI) yielded a higher value, $\mathrm{EA}(C_6F_5Cl) = 1.07$ eV, consistent with our experience that this method yields EA's that are 0.2–0.3 eV too large [1,16].

V. NEW PLASMA DECAY PHENOMENA

In a simple electron-(Ar^+, He^+) plasma, the mobile electrons are inhibited from diffusing to the walls of the flow tube by the electric field of the more massive positive ions. This ambipolar diffusion process governs the plasma decay rate as long as the plasma density is large enough that the Debye shielding length is greater than the radius of the flow tube. When C_6F_5Cl is added to the plasma, electrons begin to attach, forming only $C_6F_5Cl^-$ at low temperatures. Negative ions are trapped in the space charge field of the positive ions,

along the axis of the cylindrical plasma, until the electron density has been exhausted through attachment and ambipolar diffusion. At this point, the transition from an electron/positive-ion plasma to a negative-ion/positive-ion plasma is quite sharp, occurring over a distance of about 0.5 cm along the flow tube axis or in a time span of 50 μs and is quite evident in the Langmuir probe current-voltage characteristics following the collapse of the electron density in the plasma [7]. The sharp transition between electron-ion and ion-ion ambipolar diffusion was first observed experimentally by Lineberger and Puckett, in 1969 [19].

One complication to this picture emerges because of the simultaneous conversion of Ar^+ and He^+ to heavier positive ions through charge transfer reactions—usually at a much slower rate ($\sim 10^{-9}$ cm^3 s^{-1}) than the electron attachment process ($\sim 10^{-7}$ cm^3 s^{-1}). The lighter positive ions presumably account for most of the diffusion of positive ions to the walls of the flow tube. There seems to be a sudden transition from ambipolar diffusion of electrons and light positive ions to ambipolar diffusion of electrons and heavy positive ions. An example of such a sharp transition was shown in an earlier work with the FALP [20], where the electron attachment rate constant (to PF_5) was small enough that a relatively large concentration of reactant was required, and hence a larger concentration of heavy positive ions obtained. This effect is unnoticeable in the present work with the C_6F_5X because the electron attachment rate constants are large.

A new plasma effect was observed in the present work but is not well understood. We observe a sudden transition from the attachment-detachment near-steady state to a more rapidly decaying electron concentration, as seen in Fig. 4. The effect is apparently due to the continual release of fresh electrons by $C_6F_5Cl^-$ from the heart of the plasma. For electron attachment to C_6F_5Cl at elevated temperatures, both light (Cl^-, 35.5 amu) and heavy ($C_6F_5Cl^-$, 202.5 amu) anions were produced in the electron attachment. For this discussion we shall ignore the small fraction of $C_6F_5^-$ anions that were observed in the mass spectra and which are suspected due to impurities. The nondetaching Cl^- concentration builds up continuously in the core of the plasma while electrons supply the diffusive loss of negative charge to the walls of the flow tube. Figure 4 shows the axial concentration of Cl^-. It is assumed that the massive $C_6F_5Cl^-$ ions are relegated to life closer to the axis of the cylindrical plasma. As shown in Fig. 4 (and evident in all of the data above about 500 K), there is a sudden transition in the electron density decay rate while there are still copious electrons in the plasma, with the result that the electron density drops as if the diffusion rate had approximately doubled.

The precise explanation for this transition eludes us, as the modeling shown in Fig. 4 fails to reproduce the sudden transition. The transition point occurs when the electron density is still a significant fraction (0.1–0.4) of the total negative charge density, well ahead of the point where the electron-ion plasma collapses into the ion-ion mode. Two attempts have been made to model this transition by modifying the rate equations [10] to account for the presence of detaching and nondetaching anions in the plasma. The first is to (a) assign branching fractions to Cl^- and $C_6F_5Cl^-$ products upon electron attachment and then (b) allow the $C_6F_5Cl^-$ to detach, but not the Cl^-. The electrons and positive ions continue to control the ambipolar diffusion rate. Using the one-dimensional rate equations for charged particle concentrations along the flow tube axis,

$$\delta n_{1-}/\delta t = f_1 k_a n_r n_e - k_d n_{1-}, \tag{6}$$

$$\delta n_{2-}/\delta t = f_2 k_a n_r n_e, \tag{7}$$

$$\delta n_+/\delta t = -\nu_D n_+, \tag{8}$$

$$\delta n_e/\delta t = (\delta n_+/\delta t) - (\delta n_{1-}/\delta t) - (\delta n_{2-}/\delta t), \tag{9}$$

where t is the reaction time along the flow tube axis, n_{1-} is the $C_6F_5Cl^-$ concentration and f_1 its branching fraction, n_{2-} is the Cl^- concentration and f_2 its branching fraction (and $f_1+f_2=1$), and n_e, n_+, and n_r are the electron, positive ion, and reactant concentrations, respectively. The final equation is a statement of plasma neutrality. In applying solutions of these one-dimensional rate equations to data such as given in Fig. 4, one may choose branching fractions which yield an electron density decay curve which approximates the experimental data, but without the sharp break at long times. Operationally, one may find branching fractions which reproduce the late drop in the electron density, but with a decline that begins sooner than observed. Or one may find slightly different branching fractions which fit the early and middle portions of the electron density curve, but do not allow the electron density to drop off at long times as fast as do the data.

A second approach embodies the first and includes an increase in the ambipolar diffusion rate beginning at the point where the sharp break is observed, as shown in Fig. 8. In this approach, the location of the sharp break and the resulting increase in the diffusion rate are both treated simply as fitting parameters, so it is no surprise that good fits to the data may be obtained. However, this sudden increase in the diffusion rate is of unknown origin, though we assume it has to do with the continual release of electrons by $C_6F_5Cl^-$ in the core of the plasma. A hand-waving explanation is that the radial distribution of negative charge consists of heavy $C_6F_5Cl^-$ ions near the plasma axis, light Cl^- ions tending to lie further out, and electrons dominating the distribution at large radius. The $C_6F_5Cl^-$ ions release electrons near the plasma axis, and it is hypothesized that these electrons require longer to diffuse to the outer reaches of the plasma. The results may be complicated further by the conversion of light positive ions (He^+ and Ar^+) to more massive ones ($C_6F_5Cl^+$ and dissociation fragments). This proposed effect results in (a) a slower transition from electron-ion plasma to ion-ion plasma (300 instead of 50 μs) and (b) increases the probability that an electron already near the boundary of the plasma will diffuse to the walls. Only a two-dimensional model of the plasma reactions and diffusion can answer this question definitively, by modeling data such as shown in Fig. 8 with physically meaningful parameters.

VI. COMPUTATIONAL METHODS AND RESULTS

Density functional theory (DFT) and the Møller-Plesset perturbation theory (MP2) method were applied to C_6F_5Cl

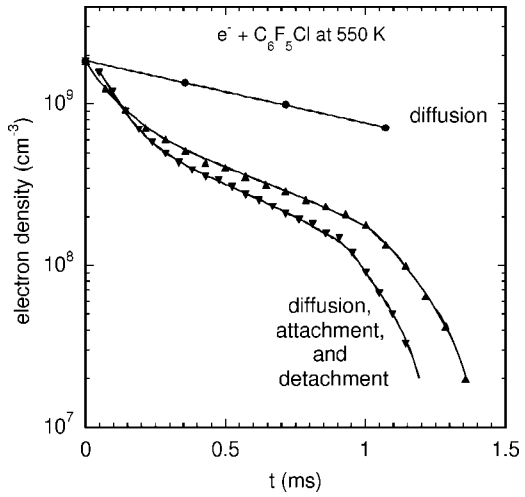

FIG. 8. Electron attachment-detachment data (triangles) for C_6F_5Cl at 550 K, for C_6F_5Cl concentrations of 5.28×10^{10} cm^{-3} (upper triangles) and 8.80×10^{10} cm^{-3} (lower triangles). The best-fit curves were obtained with $k_a=9.59\times10^{-8}$ cm^{-3} s^{-1} and $k_d=4140$ s^{-1} and a branching fraction for the $C_6F_5Cl^-$ ion product of 0.87. The ambipolar diffusion decay rate is $\nu_D=869$ s^{-1} (topmost points), measured in the absence of C_6F_5Cl, but a higher (artificial) diffusion decay rate of 1300 s^{-1} was used to fit the drop that occurs around ~1 ms reaction time. Both the transition time and the high diffusion rate were treated as fitting parameters.

and C_6F_5Br to determine structures and energetics for the neutrals and anions and to obtain thermodynamic quantities needed for interpretation of the attachment and detachment results for C_6F_5Cl. The GAUSSIAN-03 program was used for this work [21]. The computations were carried out on a personal computer and on an IBM SP/RS6000 computer at the Maui High Performance Computing Center. DFT [specifically, the Becke three-parameter–Lee-Yang-Parr (B3LYP) hybrid functional] [22,23] was used to calculate entropies and heat capacities because it was feasible to use a larger Gaussian basis set [6-311+G(3df)] than with MP2 methods. All wave functions were checked for stability—i.e., that the molecular orbital set chosen was the lowest-energy one. The G3(MP2) compound method [24] was used to determine an accurate $EA(C_6F_5Cl)$. The G3(MP2) method is not applicable to atoms larger than Ar, so we applied the G2(MP2) method [25] to C_6F_5Br. C_6F_5I was not treated computationally because the basis sets used in this work are not applicable to the I atom. The G3(MP2) and G2(MP2) methods utilize scaled zero-point energies (ZPE's) calculated at the HF/6-31G(d) (Hartree-Fock) level of theory. An approximation had to be made for the HF ZPE of $C_6F_5Cl^-$, because we were unable to locate a stable HF structure despite many attempted distortions of the neutral structure. In order to estimate the anion ZPE needed to adjust the G3(MP2) total energy to 0 K, we calculated vibrational frequencies for C_6F_5Cl neutral and anion using MP2 and B3LYP theory with several basis sets [26]. We considered several strategies for using this information and ended up simply using the average values, scaled by standard factors [27], together with a correction factor determined by comparison with the HF ZPE for the neutral, to estimate that the $C_6F_5Cl^-$ HF ZPE is 0.04585 ± 0.00070 hartree. A similar procedure was likewise necessary for $C_6F_5Br^-$. We leave to philosophers the implications of deducing a HF ZPE for (possibly) nonexistent HF structures.

The various calculated quantities are given in Table III. The resulting (approximate) G3(MP2) $EA(C_6F_5Cl)$ is 0.728 eV, a result that carries an uncertainty of ±19 meV in addition to the usual error limits for the G3(MP2) method [28] (±57 meV on average). The G2(MP2) method is only slightly less accurate (±68 meV on average). However, application to a Br-containing molecule introduces additional uncertainty because relativistic effects are significant. At best, the nonrelativistic treatment yields an average total energy between the spin-orbit levels of the anion ground state, meaning that the true $EA(C_6F_5Br)$ is probably larger than G2(MP2) indicates (0.923 eV). If the spin-orbit splitting in the BrO^- case [28] is taken as a guide, one would have to add roughly 0.06 eV to the calculated $EA(C_6F_5Br)$, moving the G2(MP2) EA value closer to the experimental result of Dillow and Kebarle [2]. But the G2(MP2) result for $EA(C_6F_5Cl)$ implies that the accuracy of the G2(MP2) method is already reduced over that of G3(MP2), even for second-row atoms.

The DFT method [B3LYP/6-311+G(3df)] yielded $EA(C_6F_5Cl)=1.069$ eV. In our experience [1,16], this method yields EA's that are 0.2–0.3 eV too high, so the DFT result implies to us a value of $EA(C_6F_5Cl)$ in the range 0.77–0.87 eV, which is in reasonable agreement with the G2(MP2) result and with our experimental value and that of Dillow and Kebarle [2]. The analogous DFT result for $EA(C_6F_5Br)$ is 1.429 eV. We thus expect the true $EA(C_6F_5Br)$ to be in the range 1.13–1.23 eV, in good agreement with Dillow and Kebarle's experimental value (1.15 eV) [2], though, again, relativistic effects for a Br-containing molecule introduce additional uncertainty in this result.

MP2 and DFT structures are shown in Fig. 9 for C_6F_5Cl and in Fig. 10 for C_6F_5Br neutrals and anions. Figure 10 shows an interesting and unresolved issue: for $C_6F_5Cl^-$, both the MP2 and DFT geometry optimizations placed the Cl atom significantly out of plane. But for $C_6F_5Br^-$, the DFT optimization yielded a planar anion, while the MP2 one placed the Br atom far out of plane. (This distortion also displaces the other atoms slightly, so by "plane" we mean the average plane of the remaining atoms.) Thus, the $C_6F_5Br^-$ point group and state is $C_{2v}(^2A_1)$ for DFT and $C_s(^2A')$ for MP2. Based on previous experience comparing DFT and MP2 structures, we suspect that the Br atom in fact lies out of plane.

VII. CONCLUSIONS

We have measured electron attachment rate constants and product branching fractions for C_6F_5Cl, C_6F_5Br, and C_6F_5I, and electron detachment rate constants for $C_6F_5Cl^-$, over the temperature range 300–550 K (Table I). The C_6F_5Cl case was especially interesting because electron attachment to C_6F_5Cl was found to yield not only the parent anion but also

TABLE III. Results of Møller-Plesset and density functional calculations for C_6F_5X, in hartree units except where indicated.

Quantity	C_6F_5Cl (C_{2v}, $^1A_1$)	$C_6F_5Cl^-$ (C_s, $^2A'$)	C_6F_5Br (C_{2v}, $^1A_1$)	$C_6F_5Br^-$ (C_s, $^2A_1$)[a]
HF ZPE[b]	0.04892	0.04585		
DFT ZPE[c]	0.05017	0.04648	0.04852	0.04570
G3(MP2) (0 K)[d]	−1186.75820	−1186.78497		
G2(MP2) (0 K)[d]	−1186.65413	−1186.67622	−3299.49083	−3299.52475
DFT (0 K)[e]	−1188.23437	−1188.27368	−3302.15410	−3302.20661
G3(MP2) EA[f]	0.728 eV			
G2(MP2) EA[f]	0.601 eV		0.923 eV	
DFT EA[f]	1.069 eV		1.429 eV	
DFT EA adjusted[g]	0.82 eV		1.18 eV	
Expt. (ion equilibria)	0.82±0.11 eV		1.15±0.11 eV	
Expt. (present)	0.75±0.08 eV			

[a]The geometry of $C_6F_5Br^-$ is C_s symmetry for MP2 optimization and C_{2v} for DFT optimization.
[b]HF/6-31G(d) level of theory, scaled by 0.8929, for G3(MP2) results. The HF ZPE for $C_6F_5Cl^-$ and $C_6F_5Br^-$ had to be estimated from ZPE's at other levels of theory, and this estimate adds an uncertainty of 19 meV to the usual G3(MP2) and G2(MP2) error limits; see Sec. VI.
[c]B3LYP/6-311+G(3df) level of theory, scaled by 0.989.
[d]Total energy at 0 K using the G3(MP2) or G2(MP2) formalism.
[e]B3LYP/6-31+G(3df)//B3LYP/6-31+G(3df)+ZPE.
[f]Difference between the total energy of the neutral at 0 K minus that of the anion.
[g]Experience has shown that the correct EA is about 0.25 eV lower than obtained with this method, and the uncertainty in the adjusted EA is ±0.25 eV.

Cl^- at elevated temperatures. This is the first case we know of where a detaching product ion competes with a nondetaching one. The result is that the concentration of the nondetaching product ion (Cl^-) builds up in the electron-ion plasma with time, while that of the detaching one ($C_6F_5Cl^-$) decreases in time. A simple mass spectrometric determination of the product branching fractions at long times would thus give an erroneous result.

A new plasma decay effect was noted as a result of having the two types of negative ions trapped in the space charge field of the positive ions in the electron-ion plasma. We hypothesize that electrons thermally detached from the $C_6F_5Cl^-$ near the core of the cylindrical plasma cause a delay in the collapse of the electron-ion plasma to an ion-ion one. At high temperatures, a sudden transition in the plasma decay rate was observed, well before the electron concentration dropped to zero.

$EA(C_6F_5Cl) = 0.75\ eV \pm 0.08\ eV$ was deduced from the attachment-detachment results (Table II). This value is in

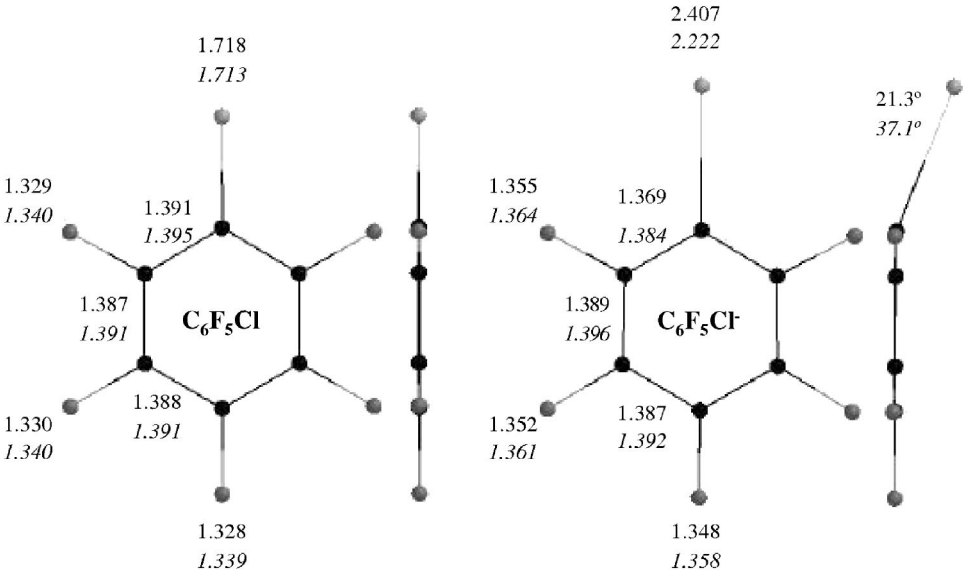

FIG. 9. Optimized structures for C_6F_5Cl (C_{2v}, $^2A_1$) and $C_6F_5Cl^-$ (C_s, $^2A'$). Both are shown perpendicular and parallel to the molecular plane, with the Cl atom at the top of the figure. The bond lengths and angle in plain type are from B3LYP/6-311+G(3df) optimizations. Those in italics are the optimized MP2(full)/6-31G(d) geometries used in the G3(MP2) calculation. The angle given is for C_4-C_1-Cl.

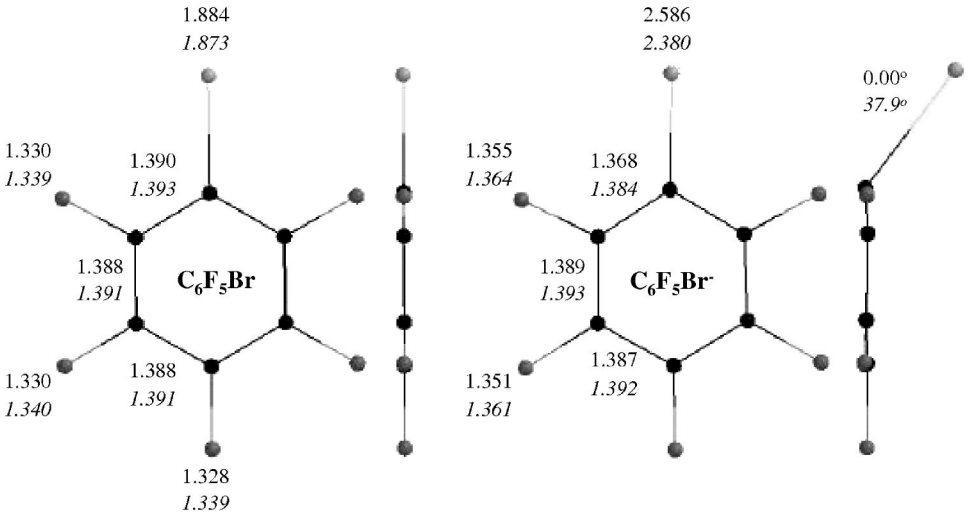

FIG. 10. Optimized structures for C_6F_5Br (C_{2v}, $^2A_1$) and $C_6F_5Br^-$ (C_s, $^2A'$ for MP2 and C_{2v}, $^2A_1$ for DFT). Both are shown perpendicular and parallel to the molecular plane, with the Br atom at the top of the figure. The bond lengths and angle in plain type are from B3LYP/6-311+G(3df) optimizations. Those in italics are the optimized MP2(full)/6-31G(d) geometries used in the G2(MP2) calculation. DFT gives $C_6F_5Br^-$ as planar. The angle given is for C_4-C_1-Cl

agreement with that measured by Dillow and Kebarle using ion equilibria [2].

We carried out a G3(MP2) calculation of EA(C_6F_5Cl) and obtained 0.728 eV (Table III), which is also in agreement with the experimental values within the maximum expected computational uncertainty of 0.1 eV. A G2(MP2) calculation yielded EA(C_6F_5Br)=0.923 eV [and EA(C_6F_5Cl) =0.601 eV]. It is estimated that a relativistic calculation would increase the calculated EA(C_6F_5Br) enough that it could be said to be in agreement with experiment. Structures for the C_6F_5Cl and C_6F_5Br neutrals and anions were optimized using both MP2 and DFT methods. There is an interesting discrepancy for $C_6F_5Br^-$: the MP2 optimization shows the Br atom to be out of plane in the anion, while the DFT optimization indicates that the molecule is planar. For $C_6F_5Cl^-$, both methods give the same basic structure, differing most noticeably in the exact angle for which the Cl atom protrudes above the average plane of the remainder of the molecule.

ACKNOWLEDGMENTS

We are grateful for the support of the Air Force Office of Scientific Research for this work. T.M.M. is under contract (No. F19628-99-C-0069) with Visidyne, Inc., Burlington, MA. This work was supported in part by a grant of computer time from the DOD High Performance Computing Modernization Program at the Maui High Performance Computing Center.

[1] T. M. Miller, J. M. Van Doren, and A. A. Viggiano, Int. J. Mass Spectrom. Ion Processes **233**, 67 (2004).
[2] G. W. Dillow and P. Kebarle, J. Am. Chem. Soc. **111**, 5592 (1989).
[3] W. T. Naff, R. N. Compton, and C. D. Cooper, J. Chem. Phys. **54**, 212 (1971).
[4] C. R. Herd, N. G. Adams, and D. Smith, Int. J. Mass Spectrom. Ion Processes **87**, 331 (1989).
[5] H. Shimamori, T. Sunagawa, Y. Ogawa, and Y. Tatsumi, Chem. Phys. Lett. **227**, 609 (1994).
[6] S. Nakagawa, Chem. Phys. **282**, 127 (2002).
[7] D. Smith and P. Španěl, Adv. At., Mol., Opt. Phys. **32**, 307 (1994).
[8] T. M. Miller, A. E. S. Miller, J. F. Paulson, and X. Liu, J. Chem. Phys. **100**, 8841 (1994).
[9] The C_6F_5X were purchased from Aldrich Chemicals and stated to be >99% pure. Approximate vapor pressures we observed while preparing mixtures in He were 8.6 kPa (C_6F_5Cl, 300 K), 0.89 kPa (C_6F_5Br, 297 K), and 0.28 kPa (C_6F_5I, 297 K).
[10] T. M. Miller, R. A. Morris, A. E. S. Miller, A. A. Viggiano, and J. F. Paulson, Int. J. Mass Spectrom. Ion Processes **135**, 195 (1994).
[11] U. Berzinsh, M. Gustafsson, D. Hanstorp, A. E. Klinkmueller, U. Ljungblad, and A.-M. Maartensson-Pendrill, Phys. Rev. A **51**, 231 (1995).
[12] H.-P. Fenzlaff and E. Illenberger, Int. J. Mass Spectrom. Ion Processes **59**, 185 (1984).
[13] Q.-s. Li, X.-j. Feng, Y. Xie, and H. F. Schaefer III, J. Phys. Chem. A **108**, 7071 (2004).
[14] C. E. Klots, Chem. Phys. Lett. **38**, 61 (1976). Polarizabilities were taken from the B3LYP/6-311+G(3df) calculations described in Sec. IV: 12.86 Å^3 for C_6F_5Cl, 13.98 Å^3 for C_6F_5Br, and from these we estimated 14.9 Å^3 for C_6F_5I.
[15] D. F. McMillen and D. M. Golden, Annu. Rev. Phys. Chem. **33**, 493 (1982).
[16] T. M. Miller, J. F. Friedman, and A. A. Viggiano, J. Chem. Phys. **120**, 7024 (2004).
[17] M. W. Chase, C. A. Davies, J. R. Downey, D. J. Frurip, R. A. McDonald, and A. N. Syverud, JANAF Thermochemical Tables, 3rd ed. [J. Phys. Chem. Ref. Data **14**, Suppl.No. 1, 1, (1986)].
[18] T. M. Miller, S. T. Arnold, and A. A. Viggiano, Int. J. Mass Spectrom. Ion Processes **227**, 413 (2003).
[19] W. C. Lineberger and L. J. Puckett, Phys. Rev. **186**, 116

(1969).
[20] T. M. Miller, J. F. Friedman, A. E. S. Miller, and J. F. Paulson, Int. J. Mass Spectrom. Ion Processes **149/150**, 111 (1995).
[21] M. J. Frisch *et al.*, *GAUSSIAN 03, Revision B.02*, (Gaussian, Inc., Pittsburgh, 2003).
[22] A. D. Becke, J. Chem. Phys. **98**, 5648 (1993).
[23] J. P. Perdew, K. Burke, and Y. Wang, Phys. Rev. B **54**, 16533 (1993); K. Burke, J. P. Perdew, and Y. Wang, in *Electron Density Functional Theory: Recent Progress and New Directions*, edited by J. F. Dobson, G. Vignale, and M. P. Das (Plenum, New York, 1998).
[24] L. A. Curtiss, P. C. Redfern, K. Raghavachari, V. Rassolov, and J. A. Pople, J. Chem. Phys. **110**, 4703 (1999).
[25] L. A. Curtiss, K. Raghavachari, and J. A. Pople, J. Chem. Phys. **98**, 1293 (1993).
[26] ZPE values were calculated at the MP2(Full)/6-31G(d) level of theory (50.44, 48.51 mhartree, for C_6F_5Cl neutral and anion, respectively), MP2(FC)/6-31G (48.13, 45.37 mhartree), and with the B3LYP method using basis sets 3-21G (51.64, 48.09 mhartree), 6-31G (49.99, 46.73 mhartree), 6-31G(d) (50.16, 47.02 mhartree), and 6-311+G(3df) (50.73, 47.00 mhartree). In each case, of necessity, the geometries were optimized at the same level of theory.
[27] J. B. Foresman and Æleen Frisch, *Exploring Chemistry with Electronic Structure Methods*, 2nd ed. (Gaussian, Pittsburgh, 1996), p. 64.
[28] M. K. Gilles, M. L. Polak, and W. C. Lineberger, J. Chem. Phys. **96**, 8012 (1992).